Measurement 148 (2019) 106922

Contents lists available at ScienceDirect

Measurement

journal homepage: www.elsevier.com/locate/measurement

Rail foot flaw detection based on a laser induced ultrasonic guided wave method ☆

Madhuri Pathak *, Sanath Alahakoon, Maksym Spiryagin, Colin Cole

Centre for Railway Engineering, Central Queensland University, North Rockhampton, QLD, Australia

ARTICLE INFO

Article history:
Received 14 May 2019
Received in revised form 8 July 2019
Accepted 3 August 2019
Available online 7 August 2019

Keywords:
Rail foot flaw detection
Finite element simulation
Ultrasonic guided wave
Laser induced ultrasound
Non-contact
Non-destructive

ABSTRACT

With the advancements in Railway Engineering in non-destructive testing technologies, a system for the fast detection of rail flaws at earliest stage is in huge demand. Such a system could result in savings in maintenance and would have less operational impact. Most of the research work in this area has been carried out for the defects in rail head and web, while defects in rail foot, which are difficult to access are responsible for derailments and accidents. This research work is focusing on detecting rail foot flaws using non-destructive, non-contact laser induced ultrasonic guided wave-based technique. This paper presents a conceptual technique based on finite element simulations of the propagation of laser induced ultrasonic guided waves to detect cracks in the rail foot. The simulations are performed at different frequencies and varying sensor positions to identify the best suited frequency and sensor location on locomotive for reliable defect detection.

1. Introduction

RAIL flaw detection plays an important role in context of primary concerns of heavy haul Railway Engineering for safety and reliable tonnage rail transportation [1,2]. Early detection of cracks can prevent derailments, serious injuries to personnel and inherent economic losses owing to railway accidents occurring due to rail breakages [3,4,5]. Various conventional techniques have previously been used for the purpose of rail flaw detection such as dye penetration testing, vibration measurement, alternating current field measurement and acoustic techniques. On account of the fact that these methods need some contact with the rail surface, they could not be used in mobile crack detection systems [6,7]. Inevitably, this disadvantage of the time consuming conventional methods led to the development of laser induced ultrasonic guided wave based crack detection, which does not require any contact with the rail surface, while testing [8,9]. Moreover, there has been research carried out for crack detection using eddy current technology for inspection speed up to 150 m/s for material with less mass density such as wires, tubes and bars [10] but not for the rail foot.

The proposed method consists of a pulsed laser injection system, air coupled sensor bank and its positioning system, digital signal processing unit, a computer and data storage system which will be mounted on a locomotive. The locomotive is believed to be an ideal location for mounting these devices as they need an external power supply unit. Certainly, there is an inherent disadvantage of the non-contact type of non-destructive testing technologies in having a low signal to noise ratio, as there are issues related to impedance mismatch and loss of signal strength in the air [11,12]. However, this could be improved with some post signal processing methodologies to reduce noise further, which will be considered and addressed in future part of research work. Laser induced ultrasonic techniques offer an additional advantage of detecting subsurface cracks throughout the entire section of the rail, which can cover head, web and foot of the rail for crack detection subject to the excitation of the guided wave [8].

This paper first presents the concept of laser induced ultrasound guided wave-based rail foot flaw detection. This is followed by a mathematical insight into ultrasound wave propagation and excitation modes of a steel specimen. Moreover, this paper presents finite element simulations to study the behavior of laser induced ultrasonic guided waves for rail foot flaw detection. Finite element simulations will help to understand the effect of excitation frequency on wave propagation which will further help to decide the installation locations of the laser source and sensor on the locomotive. In addition, finite element simulations will be helpful to decide the equipment specification. Different excitation signal

☆ This work was supported by the Australasian Centre for Rail Innovation as part of their Project – "Moving Vehicle Rail Foot Flaw Detection."

* Corresponding author.
E-mail addresses: m.pathak@cqu.edu.au (M. Pathak), s.alahakoon@cqu.edu.au (S. Alahakoon), c.cole@cqu.edu.au (C. Cole).

https://doi.org/10.1016/j.measurement.2019.106922
0263-2241/

frequencies and different sensor positions are used to identify the best signal frequency and sensor position for reliable crack detection through finite element simulations.

The concept of laser ultrasonic based flaw detection is presented in Section 2. Section 3 presents literature review. The methodology is presented in Section 4. Section 5 presents fundamentals of ultrasonic wave propagation. Finite element modelling is presented in Section 6. Results are presented in Section 7. Discussion is presented in Section 8. Section 9 covers the conclusion and Section 10 presents future work.

2. Concept of laser ultrasonic based rail flaw detection

When high energy laser pulses are applied to the rail surface, the ultrasonic waves in the frequency range of 20 kHz to a few GHz propagate in the longitudinal direction along the rail. When these waves, which are of an elastic nature, meet any deformity or crack in the rail, they reflected back and scatter and carries signature of geometry and elastic properties of media.

These reflected waves, when sensed through air coupled sensors, give an indication of the presence of rail flaws [8,9,13]. The high energy pulses from the laser source disturb the particles near the crack vicinity, which results in vibration of crack surfaces and hence develops heat near the crack [14,15]. This phenomenon of generating heat near the crack can also be used to further enhance thermal imaging for crack detection, which is another non-contact type rail flaw detection method [14,16].

The main aim of this research is to develop this technology to be deployed in heavy haul rail networks to detect flaws in the rail track at regular train operating speeds. This testing system is best suited for being mounted on locomotives rather than on wagons, as there exists the requirement of an external power supply for the laser source and other subsystems. This research work is also aimed at investigating questions such as what would be the best installation point for the laser source on a locomotive and what would be the appropriate distance between the laser source and air-coupled ultrasonic sensors when they are mounted as an integrated testing system on a locomotive?

3. Literature review

Over the past few years, laser induced ultrasonics has been successfully applied in the fields of material thickness measurement, material characterization, laser cutting machines and medical technology [3,9,12,17]. Commercially, use of laser ultrasonics is in the frequency range of 50 kHz to 20 MHz [8]. Laser induced ultrasonic waves could propagate to longer distances if the frequencies are limited in the kHz range, while wave travel is only limited to a few millimeters in the MHz frequency range. However, the distance travelled by the wave also depends upon the physical properties of the medium such as density and Poisson's ratio [8,18,19]. For non-destructive testing, the use of laser ultrasonic waves also depends upon the power density of the laser source. It is recommended that the power density of laser ultrasonics should be in the range of 10^4–10^6 W/cm^2 for any thermo-elastic regime application, whereas it can be used up to a power density of 10 MW/cm^2 for ablation or destructive regime applications. Considering frequency parameters, most ultrasonic non-destructive testing is carried out within the 1–5 MHz range. Nd:YAG (Neodymium Yttrium Garnet) and CO_2 lasers [8,9] are the most common lasers used for the generation of laser ultrasonics. For a pulse width of 15 ns, the energy level of an Nd:YAG laser is 0.1 J considering a beam diameter of 4–8 mm which is normally used for non-destructive testing [8,9]. The generation and detection systems of any laser ultrasonic testing system are the two most important components of the whole testing unit. To generate laser induced ultrasonic waves, a short pulse of the order of nanoseconds and having a wavelength of a few nanometers (532 nm or 1064 nm) with a frequency range varying from kHz to GHz is applied to the rail specimen under test [8]. The basic principle of the generation of laser ultrasound is heating the object by applying a laser beam either in the thermo-elastic regime (can be used for non-destructive applications resulting in no damage to the material) or in the ablation regime (used for destructive testing which results in evaporation of the material from the surface). For detection of laser ultrasonic waves, contact type techniques such as the Fabry-Perot vibrometer are used, which measure the vibrations in the medium after excitation by the laser source [8,20,21]. There are some non-contact type detection methods for laser ultrasound such as electromagnetic acoustic transducers (EMATs) and air coupled transducers in the frequency range of 1–2 MHz [8,22]. For the proposed locomotive mounted system, air coupled ultrasonic transducers will be used as they do not need any contact or medium to capture the waves reflected from a crack [23,24].

4. Methodology

For this research work, finite element software is used for studying the amplitude and frequency parameters which can produce changes in physical parameters of wave propagation such as distance travelled by the waves and its attenuation.

The proposed method of a mobile rail foot crack detection system using laser induced ultrasonic guide wave technology is shown in Fig. 1.

The methodology involves the identification of excitation frequency of laser source by varying the excitation frequency. These varied frequency signals will interact in a unique way after the interaction with the crack at the rail foot. Hence, the reflections from the crack will be different, considering the fact that the distance travelled by the ultrasonic guided wave depends upon the frequency of excitation. This will help to identify the specification of the laser source to be used for the prototype at the later stage of research work. Moreover, the positioning of air coupled ultrasonic sensors, which is represented as offset with the defect in Fig. 1 also plays a crucial role in crack detection as it may affect the analysis of crack presence from the reflection of ultrasonic guided wave. This is so because the wave may either get attenuated or there could be other reflections from the edge of the rail foot, which the sensor may capture if not positioned correctly and hence affect the analysis of crack detection. A clear overview of the methodology adopted for this research work is depicted through the block diagram in Fig. 2.

The excitation frequency and sensor position analyzed through simulations will be helpful in developing prototype and experimental verifications. The conceptual design of the proposed system is shown in Fig. 3.

5. Fundamentals of wave propagation

For studying the ultrasonic wave generation in a steel section, a pulsed sine signal is simulated as a laser beam to generate ultra-

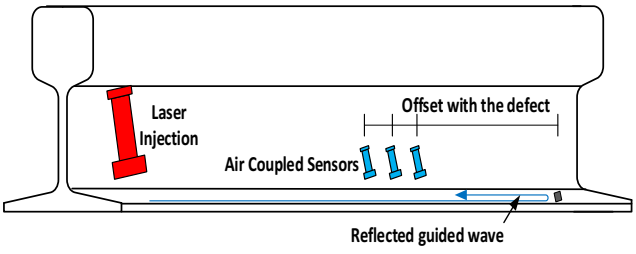

Fig. 1. Rail foot crack detection technology using laser induced ultrasound.

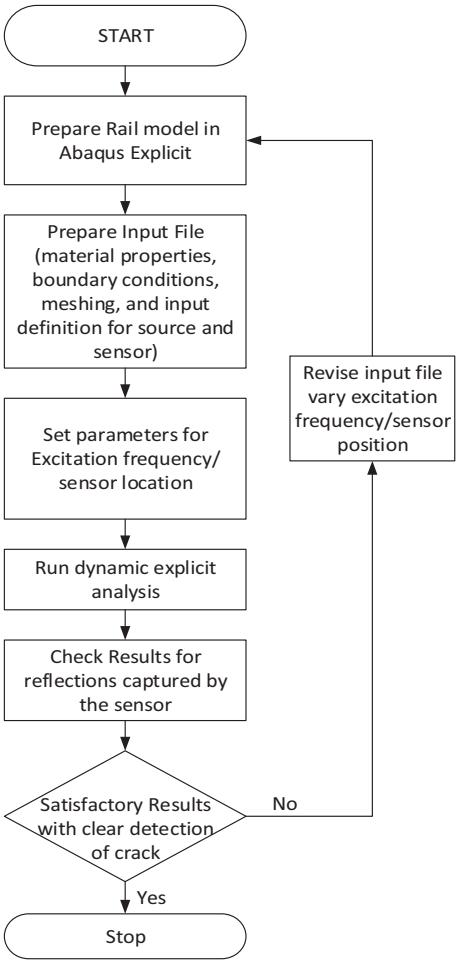

Fig. 2. Methodology adapted for the research work.

sonic guided waves in the rail foot. A pulsed sine signal of frequency f = ω/2π is simulated as representative of the laser beam applied to the rail foot. Due to the application of force, vibrations take place at the applied frequency and the equation of motion takes the form given in Eq. (1).

$$\frac{\partial^2\phi}{\partial t^2} = c^2\frac{\partial^2\phi}{\partial x^2}\frac{1}{2} \tag{1}$$

Here, $c = \omega/k$ represents velocity of wave where ω is the angular frequency, k is the wave number, and ϕ may represent any of the wave parameters such as velocity, force, pressure and displacement [25]. Considering a three-dimensional coordinate system, Eq. (1) will become:

$$\frac{\partial^2\phi}{\partial t^2} = c^2\left(\frac{\partial^2\phi}{\partial x^2}+\frac{\partial^2\phi}{\partial y^2}+\frac{\partial^2\phi}{\partial z^2}\right) \tag{2}$$

The analysis presented here considers a square steel section of 1 unit length with the excitation force wave being applied at the coordinates (0, 0) as shown in Fig. 4. A force signal, which is a source of elastic wave with amplitude A_0 can be represented as A in Eq. (3), where ω is the frequency and t is time.

Assuming that the particles of steel are vibrating in an identical manner to that of the elastic wave generated, the particle displacement A from the mean position at zero distance from the source of excitation signal (i.e. x = 0) can be represented as

$$A = A_0 \sin\omega t \tag{3}$$

Now consider the wave travelling in the z direction with the longitudinal wave velocity given by Eq. (4)

Assume that Young's Modulus $E = 210 \times 10^9$ Pa

Density $\rho = 7800$ kg/m^3

Poisson's ratio $\mu = 0.33$

Then

$$V_L = \sqrt{\frac{E(1-\mu)}{\rho(1+\mu)(1-2\mu)}} = 6315.88\ \text{m/s} \tag{4}$$

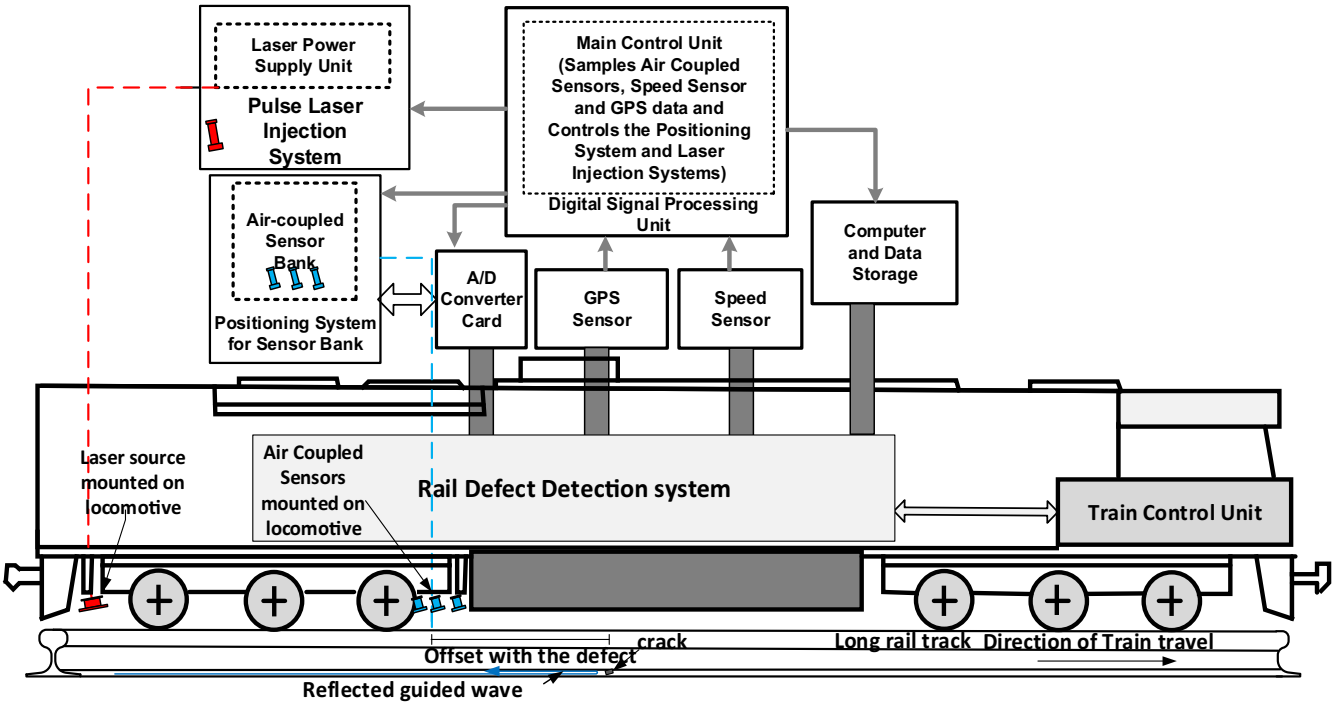

Fig. 3. Conceptual design of moving vehicle rail flaw detection system.

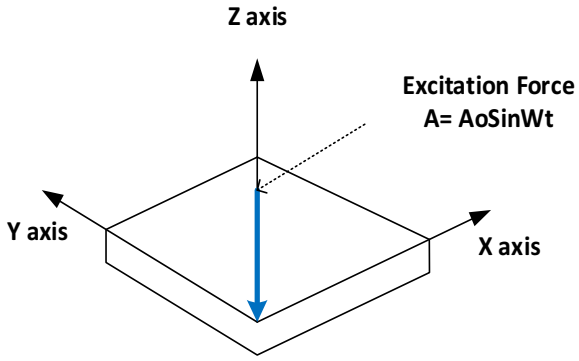

Fig. 4. Rectangular section and coordinate system.

Travelling time t' of the wave to travel a distance $\times$ can be calculated from

$$t' = x/V_L$$

The phase of the generated wave at this distance will lag behind the phase at x = 0 (source position) by an amount $\omega t'$

Then $A = A_0 \sin\omega(t - t')$

$$A = A_0 \sin\omega\left(t - \frac{x}{V_L}\right) \tag{5}$$

For a time period the waves travel by a distance

$\lambda = V_L T$, λ where is the wavelengthNow (5) can be written as

$$A = A_0 \sin 2\pi\left(\frac{t}{T} - \frac{x}{\lambda}\right)$$

$$A = A_0 \sin(\omega t - kx) \tag{6}$$

where $k = \frac{2\pi}{\lambda} = \frac{\omega}{V_L}$

The waves are disturbing particles present in the media and the velocity of waves can be considered as particle velocity [25] and it can be represented as

$$V_L(x,t) = \frac{\partial A(x,t)}{\partial t} = U$$

$$U = \frac{\partial A}{\partial t}$$

$$U = \omega A_0 \cos(\omega t - kx)$$

$$U_0 = \omega A_0$$

From Eq. (4)

$$\frac{\partial A}{\partial t} = \omega A_0 \cos(\omega t - kx)$$

$$\frac{\partial^2 A}{\partial t^2} = -\omega^2 A_0 \sin(\omega t - kx) \tag{7}$$

$$\frac{\partial^2 A}{\partial x^2} = -k^2 A_0 \sin(\omega t - kx) \tag{8}$$

Thus, from Eqs. (7) and (8),$\frac{\partial^2 A}{\partial t^2} = V_L^2 \frac{\partial^2 A}{\partial x^2}$ – Equation of motion of guided wavesIntroducing V_L in Eq. (7) results in

$$\frac{\partial^2 A}{\partial t^2} = V_L^2\left(-k^2 A_0 \sin(\omega t - kx)\right)$$

$$\frac{\partial^2 A}{\partial t^2} = -k^2 A_0 V_L^2 \sin(\omega t - kx) \tag{9}$$

Make the following substitutions

$$\frac{\partial^2 A}{\partial t^2} = -k^2 A_0 V_L^2 \sin(\omega t - kx); \quad \frac{\partial A}{\partial t} = w, \ \frac{\partial^2 A}{\partial t^2} = \frac{\partial w}{\partial t}$$

Then the wave equation with external excitation along one dimension can be re-written as a first order partial differential equation;

$$\frac{\partial w}{\partial t} = -k^2 A_0 V_L^2 \sin(\omega t - kx) + P_0 \sin(\omega t) \tag{10}$$

where P_0 is the amplitude of excitation signal

For the two-dimensional case, based on Eq. (9) the two-dimensional wave equation with external excitation can be re-written as

$$\frac{\partial w_x}{\partial t} = -k^2 A_0 V_L^2 \sin(\omega t - kx) + P_0 \sin(\omega t)$$
$$\frac{\partial w_y}{\partial t} = -k^2 A_0 V_L^2 \sin(\omega t - ky) + P_0 \sin(\omega t)$$

Ultrasonic guided waves are multimodal and dispersive in nature [26]. These waves are excited with various modes of propagation which possess different velocities. After reflection of these waves from the crack geometry, these modes get scattered and hence generate some distortion in the reflected waveforms affecting the signature analysis of the presence of cracks [27]. Different wave modes interact with the crack in a unique manner, this is the inherent disadvantage of guided waves. This makes it a complex analysis and hence it is required to understand the ultrasonic wave propagation phenomenon with different wave modes. These wave modes can be identified with their individual velocities. It is always preferable to perform the study with selected wave modes. Moreover, the defect detection using ultrasonic guided waves is sensitive to stress distribution in the media due to ultrasonic guided wave modes and frequencies [27,28]. Both of these aspects of using guided waves for non-destructive testing needs to be considered and hence will be addressed in future research work.

The above mathematical solution to the wave equation alone does not provide sufficient information on the behavior of laser induced ultrasound guided waves inside a rail foot.

Also, solution of above equations is not possible manually considering various modes of ultrasonic waves. This complexity is further increased when we consider the wave propagation in all directions. Additionally, when a finite element model is prepared for this kind of analysis, this impacts further on the time and complexity required to solve equations for each element multiplied by the number of nodes. This is the reason why finite element analysis software is used for this research work and studying ultrasonic wave behavior. However, depending on the type of model, number of finite elements, meshing size, type of element used, problem definition and type of analysis the simulation time could be different. As such further research is carried out in finite element simulation platforms, which provides some valuable information of wave reflection and other related parameters. This is presented in the following sections.

6. Finite element modelling

For studying the behavior of laser induced ultrasonic guided waves and their propagation in the rail section, a finite element simulation model is developed and is presented in this section. A numerical modelling method is implemented to study the behavior of ultrasonic waves in the rail sections using finite element software [29]. The finite element analysis utilizes a mathematical sub-domain (small element) approach to simulate the guided wave propagation in the rail section [30,29,31]. The whole geometry of the rail section is divided into small finite subdomains, which are called finite elements and are shown in Fig. 5.

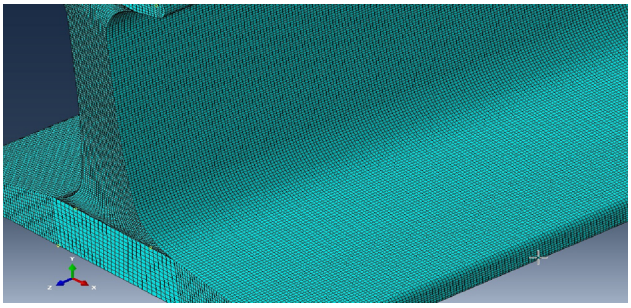

Fig. 5. Meshed rail section with C3D8 elements.

For meshing of the rail section using C3D8 elements (continuum 3D linear brick type 8 node elements), the model is partitioned into small sections [31–34]. The results will be correlated and compared with the results obtained from laboratory samples that will later be designed and built. The simulations performed involve the following steps:

1) Part geometry of the rail section is created in the software.
2) Rail geometry is partitioned into small sections.
3) Meshing the geometry into finite elements using C3D8 type of elements.
4) Assign material properties to the rail section.
5) Create and assign load for simulating laser excitation.
6) Assign boundary conditions.
7) Create and assign step input data files for output file simulation.

Table 1 presents the modelling parameters used for the finite element simulations of ultrasonic wave propagation in the rail foot.

Table 2 represents the input and output parameters used for the simulation.

A 2.4 m rail section with four supports of the dimensions $146 \times 180 \times 7.5$ mm and center to center distance of 600 mm is considered and created in Abaqus® and modelled with material properties as mentioned in Table 2. The simulation was performed in Abaqus® 2017 version and dynamic explicit analysis was performed. A vertical single cycle load of 20 t is considered on the rail head of 2.4 m rail section. Locomotive mass of 200 t (6 axles) is used in Australia for heavy haul rail, 160 t (4 axles) mass of loaded wagon and 20 t mass of empty wagon. The advantage of using Abaqus over other similar software is that it requires less disk space and hence save memory and computation costs. However, this software is more complicated and hence considered as less user friendly for meshing and requires deeper understanding of finite element modelling. Although, meshing with Abaqus® seems to be a bit difficult but it provides finer control of the elements at the particular areas of the geometry [35]. The excitation frequency is varied from 20 kHz to 200 kHz and the time period is set in the step detail of the modelling. Though, the pulse laser can generate the frequency components ranging from kHz to MHz, the rationale behind selecting the frequency range from 20 kHz to 200 MHz is that lowest frequency component will generate the waves which travels longer distance [8]. The rail model is partitioned into small sections so as to do the structural meshing with C3D8 elements with a particular size after seeding the edges. The size of the mesh element is to be considered such that the wavelength of the wave is equal to a minimum of 5 mesh elements in size to be able to simulate proper wave propagation. Assigning boundary conditions and positioning the source at one end and the sensor at various places on the rail section as shown in Fig. 6 completes the step input part of the modelling.

Table 1
Modelling parameters.

Parameters	Value
Type of material	Solid homogenous
Mass density of rail steel	7800 kg/m^3
Poisson's Ratio	0.33
Young's Modulus	210 GPa
Mesh Element	C3D8
Analysis Type	Dynamic explicit
Frequency	20 kHz

Table 2
Input/output parameters.

Specifications	Type/Value
Source Type	Nd:YAG
Wavelength	532–1064 nm
Pulse duration	4–20 ns
Beam Diameter	0–8 mm
Pulse Energy	0–82 mJ
Pulse width	0–1 mm
Output frequency range	1 kHz–1 MHz

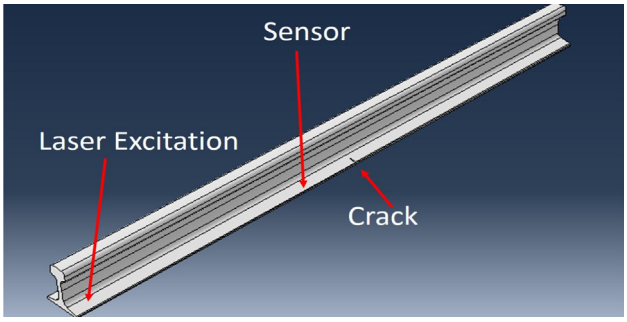

Fig. 6. Rail section with positioning of laser source, sensor and crack.

Field output and history output sections are required to be filled based on the output parameters required in the results file. The input file parameters such as displacement and time increment are provided as input to the model so as to see the variation of amplitude and frequency of waves. After checking the input file by undertaking a data check in the input processor of Abaqus®, the job is submitted for dynamic explicit analysis. After completion of the analysis, an output database file is generated with the simulated wave propagation as shown in Fig. 7.

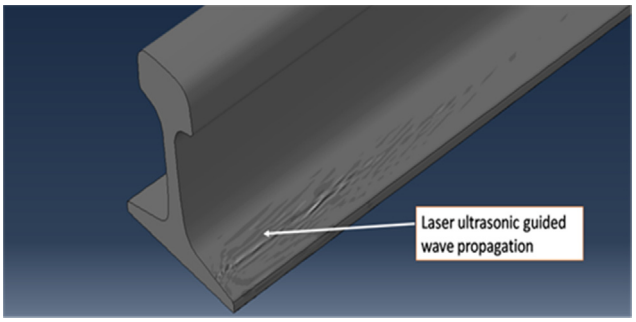

Fig. 7. Ultrasonic wave propagation through the rail foot.

6.1. Reflection of ultrasound wave at a rail foot flaw

A 2.4 m rail model is created in the software and a crack is created in the middle of the rail foot. After providing material properties and assigning section details to the rail model, a step input file is created. A load of particular amplitude and frequency is applied as a force wave to simulate the laser beam. Partitioning of the rail section is undertaken to mesh it with C3D8 type elements. Boundary conditions are applied to fix the rail foot at the bottom with fasteners and rotational motion was set as zero. The output files are created using field output and history output parameters. Then the job is submitted for a dynamic explicit type of analysis. The reflection of the guided waves from the crack in the rail sample is visible in the output of the simulation. The source is simulated to be at one end of the rail section and the sensor is placed ahead of the crack, which could detect the reflections from the crack. The simulation result for reflection of ultrasonic waves from the crack is presented in Section 7.1.

6.2. Effect of excitation frequency on wave propagation

To study the behavior of laser induced ultrasonic guided waves at excitation signals having different frequencies in the rail section, a finite element based numerical analysis is undertaken. This method has been used for investigating the behavior of laser induced ultrasonic waves on metallic and non-metallic media and in rail sections [29,36,30]. For this analysis, a rail section geometry is created in the software and then the whole geometry domain is divided into finite elements, which are called elementary sub-domains. After partitioning, meshing of the rail section is done using C3D8 elements (continuum 3D linear brick type 8 node elements) [31,32]. The analysis could also be undertaken using other type of elements such as C3D10, but the research by the authors in [37,38] suggests that the software may require a higher number of iterative equations for the solution. This could result in more simulation time for running the analysis. The 2.4 m rail section model used for the analysis is shown in Fig. 5. To identify the sensor location based on distance travelled by a laser signal a particular frequency, the following simulations were performed at different excitation frequencies. Frequency values considered for the simulations were 20 kHz, 40 kHz, 60 kHz, 100 kHz and 200 kHz. The simulation results on the effect of frequency on wave propagation will be presented in Section 7.2.

6.3. Reflected waves captured at different sensor positions

To clearly identify the crack presence, the locations of the sensor and the laser source on the moving vehicle detection system is very important. For identifying these locations, various sensor positions were considered for simulations to observe the reflected wave behavior. For every simulation, the sensor position is varied ahead of the crack such as at 2.2 m, 600 mm and 300 mm. A 2.4 m rail section is also modelled and a crack created at the middle of the rail foot. After assigning material properties of rail steel and creating a step input file with partitioning, meshing and load application, the job is submitted for explicit dynamic analysis and the reflection of the waves are observed in each simulation with the various sensor locations. The simulation results are presented in Section 7.3.

7. Simulation results

The results of all the simulations carried out for this research work are presented in this section.

7.1. Reflection of ultrasound wave at a rail foot flaw

In the initial work of this research, through the finite element simulations on a 2.4 m rail section, it is confirmed that the ultrasonic waves can propagate through the rail foot section. Also, it is observed from the result file that there were reflections from the crack geometry. The waveform of the reflection from the crack is shown in Fig. 7.

7.2. Effect of excitation frequency on wave propagation

7.2.1. Excitation signal at 20 kHz

The wave propagation is dependent upon the frequency of the applied laser signal. The time period is kept as 5e−05 s and the frequency as 20 kHz for modelling the input file in the finite element software Abaqus®. The amplitude is set as cyclic load with variable value. Dynamic explicit analysis is performed after application of load and boundary conditions, and the time and displacement values of generated ultrasonic guided waves were obtained as shown in Fig. 8. The sensor placed at the other end in the 2.4 m rail section was able to detect laser induced ultrasonic waves after 8 microseconds. Also, the reflections are observed in the waveform from the crack. The reduction in amplitude of reflected wave started at 20 μs.

7.2.2. Excitation signal at 40 kHz

The frequency for this simulation is set at 40 kHz and the time period is kept as 5e−05 s in the model tree input file. On application of laser excitation, the sensor senses the waves at approximately 4 μs and the waves started attenuating at 12.5 μs. The source is placed at one end and sensor at another end of the rail section. The time vs displacement graph is shown in Fig. 9.

7.2.3. Excitation signal at 60 kHz

For this simulation in the same rail section of 2.4 m length, frequency is set to 60 kHz to check the propagating distance and strength of reflected ultrasonic guided wave from crack. The time period is kept at 1.67e−05 s. Fig. 10 shows the time vs displacement variation of the laser generated ultrasonic guided wave in the rail section. It is clear that, for an excitation signal with frequency of 60 kHz the wave starts attenuating at 10 μs. The sensor captures the reflections in less than 2.5 μs.

7.2.4. Excitation signal at 100 kHz

For checking the behavior of the ultrasonic wave at 100 kHz the time period was set at 1e−05 s. After submitting the job for the dynamic explicit analysis, the time vs displacement curve is obtained as shown in Fig. 11. It shows that the sensor captures the ultrasonic guided wave at 2 μs. The ultrasonic waves start attenuating at 8 microseconds. The reduction in amplitude of

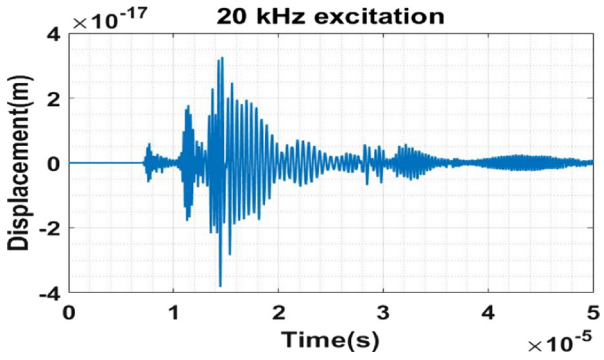

Fig. 8. Time Vs Displacement of ultrasonic guided wave at 20 kHz excitation.

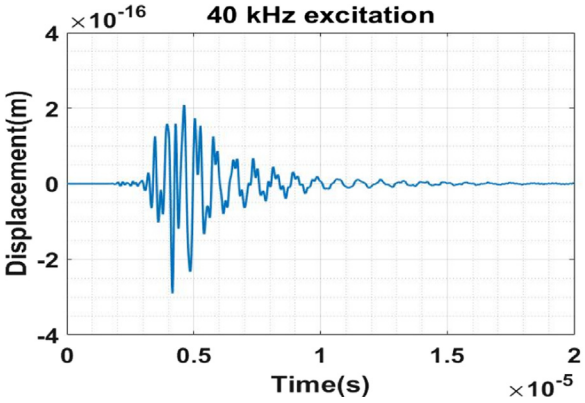

Fig. 9. Time Vs Displacement of ultrasonic guided wave at 40 kHz excitation.

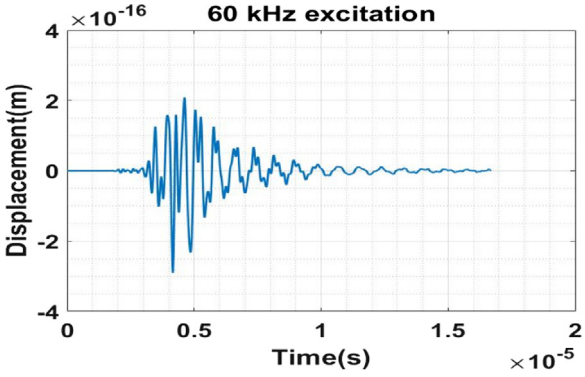

Fig. 10. Time Vs Displacement of ultrasonic guided wave at 60 kHz excitation.

reflected wave from crack with 100 kHz excitation signal is earlier when compared to reflected wave of the signal generated at 60 kHz.

7.2.5. Summarizing the results for varying excitation frequency

The finite element simulations of laser induced ultrasonic guided waves at different frequencies clearly shows through the results that the reflected wave loses its strength earliest in the form of elasticity and amplitude at the 100 kHz range frequency of excitation signal and is starting later at the minimum ultrasonic frequency of 20 kHz. This clearly shows that the ultrasonic guided wave travels longer distance with lower frequencies of ultrasonic wave. The reflected signal becomes weaker in amplitude as frequency is increased from 20 kHz to 200 kHz and hence, it is difficult to sense the reflected wave. These results are in agreement

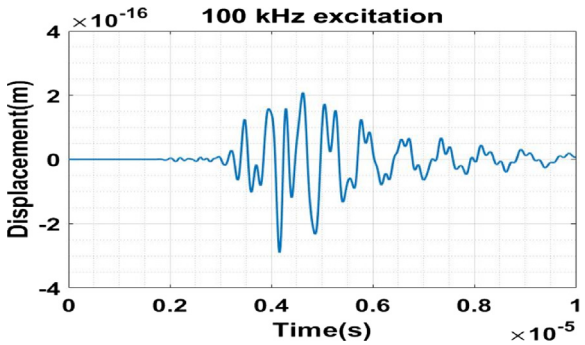

Fig. 11. Time Vs Displacement of ultrasonic guided wave at 100 kHz excitation.

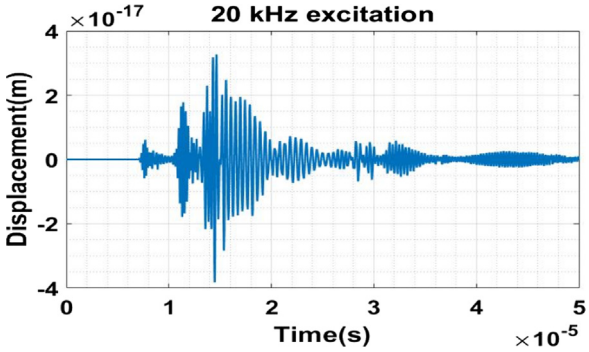

Fig. 12. Time Vs Displacement of ultrasonic guided wave when sensor is placed at 2.2 m.

with the findings of work presented in [8,9] that, with high frequency excitation, the ultrasonic guided waves attenuate faster. The results also depict that there is minimal difference in the propagating distance for the waves of 20, 40 and 60 kHz excitation signals which is also in agreement with earlier research work conducted in this area [39].

7.3. Reflected waves captured at different sensor positions

7.3.1. Sensor located at 2.2 m

The dynamic explicit analysis was undertaken for crack detection using wave propagation, keeping the sensor position at the other end of the rail section. The frequency of the excitation signal is kept at 20 kHz. The distance between the laser source and sensor was 2.2 m. The simulation for this analysis is shown in Fig. 12. The waves reached the sensor after 8 μs. There are other reflections observed in the time/displacement curve of the waveform which may be from the edge of the rail section.

7.3.2. Sensor located at 300 mm

In this simulation, the sensor was positioned 300 mm ahead of the crack. Excitation signal frequency is kept at 20 kHz. The reflected waves were observed at 5 μs which is much earlier compared to when the sensor was placed at 2.2 m. The multiple reflections are also less when the sensor is positioned ahead of the crack. Fig. 13 shows the time/displacement analysis of the simulation performed for this crack detection.

7.3.3. Sensor located at 600 mm

For this simulation the sensor was moved to 600 mm ahead of the crack, keeping the same excitation as in the previous simula-

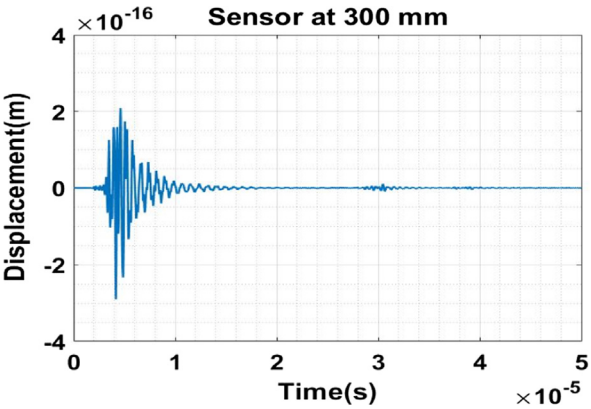

Fig. 13. Time Vs Displacement of ultrasonic guided wave when sensor placed at 300 mm.

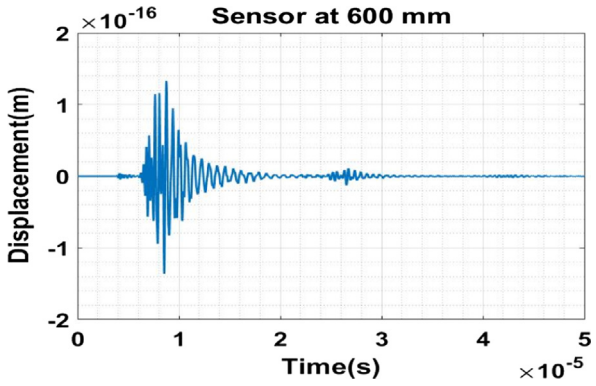

Fig. 14. Time Vs Displacement of ultrasonic guided wave when sensor placed at 600 mm.

tion. The ultrasonic guided waves reflected from the crack were detected at 9 μs. Fig. 14 shows the time Vs displacement graph.

7.3.4. Summarizing results for varying sensor positions

Results were obtained for three sensor positions at 2.2 m (at the other end of rail section), 300 mm and 600 mm ahead of the crack. The presence of the crack was detected earliest at 0.3 μs when the sensor was placed nearest to the crack at 300 mm. However, the detection was after 3 μs when the sensor was 600 mm ahead of the crack. Also, there were fewer reflections of other waves modes received at the sensor when it was placed nearer to the crack. So, it is justifiable to keep the sensor at 300 mm for this particular experimental parameter under consideration in future work.

8. Discussion

The results obtained from finite element simulations performed for different sensor locations conclude that the smaller the distance between the crack and sensor, the clearer is the signature captured by the sensor revealing the presence of the crack in the rail foot section. This is due to the fact that if the sensor is position is farther then before the reflection from the crack reaches the sensor the other reflections from the edge of the rail foot are captured by sensor and hence resulted in the faulty results as can be seen from the simulations. Also, there is another factor which shows that the reflected wave may attenuate and hence will not be able to reach up to the sensor. In addition, the sensor detects the crack earlier if positioned nearer to the crack. These results suggest keeping the minimum possible distance between crack and sensor for clear identification of cracks in the rail foot. Moreover, in regard to the selection of excitation frequency, for the particular rail section of 2.4 m length the excitation frequency was best chosen to be at 20 kHz out of the other selections. Experimental verification of these simulations will be part of future investigations. The finite element analysis is believed to be accurate and reliable for wave propagation analysis [40]. This technology is considered to be fast and capable of being used for real time applications and study. However, the simulation results presented in this research work need experimental verification considering the aspects of variations in frequency and sensor position. Further, the experimental verifications will be followed by developing the conceptual model of the mobile vehicle crack detection system to be used for rail foot flaw detection in heavy haul rail networks. This research work will facilitate decisions regarding the appropriate distance between the laser source and sensor to be mounted on the moving vehicle detection system shown in Fig. 2.

9. Conclusion

The technology of using laser induced guided wave propagation to detect cracks in rail foot sections has been verified through this research work with the help of finite element simulations. The concept of crack detection in the rail foot with the help of ultrasonic guided waves is presented in the paper along with mathematical modelling and finite element simulations. This study was required as the cracks in the rail foot is hard to detect and there has not been much research done on this area. For this purpose, the identification of excitation frequency of laser source and positioning of sensor on the locomotive is required. This is because as the distance travelled by the guided wave generated from the laser source excitation depends on the excitation frequency. Also, it was a challenge to identify the appropriate frequency of the excitation signal of the laser source, the results clearly show that the ultrasonic waves generated travel to longer distances with lower excitation frequency and they attenuate sooner with higher frequency excitation signals, which confirms the earlier theories on guided waves. The results obtained from the simulations suggests that a 20 kHz ultrasound frequency should be used for this technology of crack detection in the rail specimen of 2.4 m using laser ultrasound. The other frequencies in the simulations performed does not give satisfactory results, so the 20 kHz excitation is considered to be best suited for the purpose of this work. Moreover, the results also confirm that the location of sensor for this laboratory test specimen should be 300 mm ahead of the crack location. The results obtained through this research work will help for deciding the equipment specifications and sensor location for experimental verification of the non-destructive testing for crack detection in rail foot, which will further help in the development of prototype and field testing. However, there could be some uncertainties with the results obtained considering the presence of noise, effect of vibration in the locomotive on the excitation signal and effect of environment. All these parameters put some conceptual uncertainties at this stage of research, and these will be attended in the upcoming studies related to the project. The experimental verification of these simulation results will be undertaken as future work of this same research project.

10. Future work

Further for the future work, experimental investigations will be done, and a prototype will be developed to verify the proposed concept of crack detection in rail foot with moving vehicle. Experimental parameters and data's will be taken from this research work for the excitation frequency and positioning sensors on the locomotive. Furthermore, a virtual prototype will be developed to verify the results and an analysis on the combined uncertainty of the system will be developed. In addition, an analysis on the range of output, sensitivity and error will be checked based on the outcome of the experiments along with any uncertainties in the system.

Declaration of Competing Interest

The authors declare that they have no known competing financial interests or personal relationships that could have appeared to influence the work reported in this paper.

Acknowledgments

The author's would like to gratefully acknowledge the financial support from Australasian Centre for Rail Innovation (ACRI), Grant number: HH01B – Evaluating infrared imaging and laser ultrasonics

as detectors of rail foot flaws for project HH#1 titled "Moving Vehicle Rail Foot Flaw Detection". The author's would also like to acknowledge the support from Centre for Railway Engineering, CQUniversity and the High Performance Computing facility provided by them for this work.

References

[1] M.T. Baysari, A.S. McIntosh, J.R. Wilson, Understanding the human factors contribution to railway accidents and incidents in Australia, Accid. Anal. Prev. 40 (5) (2008) 1750–1757.
[2] G.D. Edkins, C.M. Pollock, The influence of sustained attention on railway accidents, Accid. Anal. Prev. 29 (4) (1997) 533–539.
[3] R. Clark, Rail flaw detection: overview and needs for future developments, NDT and E Int. 37 (2) (2004) 111–118.
[4] S. Alahakoon, Y.Q. Sun, M. Spiryagin, C. Cole, Rail flaw detection technologies for safer, reliable transportation: a review, J. Dyn. Syst. Meas. Contr. 140 (2) (2018) 020801.
[5] P. Wang, L. Xiong, Y. Sun, H. Wang, G. Tian, Features extraction of sensor array based PMFL technology for detection of rail cracks, Measurement 47 (2014) 613–626.
[6] B. Weekes, D.P. Almond, P. Cawley, T. Barden, Eddy-current induced thermography—probability of detection study of small fatigue cracks in steel, titanium and nickel-based superalloy, NDT and E Int. 49 (2012) 47–56.
[7] M.P. Papaelias, C. Roberts, C. Davis, A review on non-destructive evaluation of rails: state-of-the-art and future development, Proc. Inst. Mech. Eng., Part F: J. Rail Rapid Transit. 222 (4) (2008) 367–384.
[8] C.B. Scruby, L.E. Drain, Laser Ultrasonics Techniques and Applications, CRC Press, 1990.
[9] S. Davies, C. Edwards, G. Taylor, S.B. Palmer, Laser-generated ultrasound: its properties, mechanisms and multifarious applications, J. Phys. D: Appl. Phys. 26 (3) (1993) 329.
[10] J. García-Martín, J. Gómez-Gil, E. Vázquez-Sánchez, Non-destructive techniques based on eddy current testing, Sensors 11 (3) (2011) 2525–2565.
[11] J. Krautkrämer, H. Krautkrämer, Ultrasonic Testing of Materials, Springer Science & Business Media, 2013.
[12] A. Cavuto, M. Martarelli, G. Pandarese, G. Revel, E. Tomasini, Train wheel diagnostics by laser ultrasonics, Measurement 80 (2016) 99–107.
[13] A. Kromine, P. Fomitchov, S. Krishnaswamy, J. Achenbach, Scanning laser source technique for detection of surface-breaking and sub-surface cracks no. 1, in: Review of Progress in Quantitative Nondestructive Evaluation: Volume 19, AIP Publishing, 2000, pp. 335–342.
[14] F. Mabrouki, M. Thomas, M. Genest, A. Fahr, Frictional heating model for efficient use of vibrothermography, NDT and E Int. 42 (5) (2009) 345–352.
[15] R. Montanini, F. Freni, Investigation of heat generation sources in sonic infrared thermography using laser Doppler vibrometry, Proceedings of Quantitative Infrared Thermography QIRT, 2012.
[16] S.E. Burrows, A. Rashed, D.P. Almond, S. Dixon, Combined laser spot imaging thermography and ultrasonic measurements for crack detection, Nondestruct. Test. Eval. 22 (2–3) (2007) 217–227.
[17] Y. Choi, S.H. Abbas, J.-R. Lee, Aircraft integrated structural health monitoring using lasers, piezoelectricity, and fiber optics, Measurement 125 (2018) 294–302.
[18] A. Aindow, R. Dewhurst, S. Palmer, C. Scruby, Laser-based non-destructive testing techniques for the ultrasonic characterization of subsurface flaws, NDT Int. 17 (6) (1984) 329–335.
[19] R.E. Green, Non-contact ultrasonic techniques, Ultrasonics 42 (1) (2004) 9–16.
[20] J.P. Monchalin, Laser-ultrasonics: from the laboratory to industry no. 1, in: Quantitative Nondestructive Evaluation, AIP Publishing, 2004, pp. 3–31.
[21] T. Hayashi, Y. Kojika, K. Kataoka, M. Takikawa, Visualization of guided wave propagation with laser Doppler vibrometer scanning on curved surfaces no. 1, in: Review of Progress in Quantitative Nondestructive Evaluation: 34th Annual Review of Progress in Quantitative Nondestructive Evaluation, AIP Publishing, 2008, pp. 178–184.
[22] F. di Scalea, I. Bartoli, P. Rizzo, M. Fateh, High-speed defect detection in rails by noncontact guided ultrasonic testing, Transp. Res. Rec.: J. Transp. Res. Board 1916 (2005) 66–77.
[23] F. Lanza di Scalea et al., Non-contact ultrasonic inspection of rails and signal processing for automatic defect detection and classification, Insight-Non-Destruct. Test. Cond. Monit. 47 (6) (2005) 346–353.
[24] S. Dixon, S.E. Burrows, B. Dutton, Y. Fan, Detection of cracks in metal sheets using pulsed laser generated ultrasound and EMAT detection, Ultrasonics 51 (1) (2011) 7–16.
[25] J. Blitz, G. Simpson, Ultrasonic Methods of Non-Destructive Testing, Springer Science & Business Media, 1995.
[26] J.L. Rose, Ultrasonic Waves in Solid Media, ASA, 2000.
[27] P. Wilcox, M. Lowe, P. Cawley, The effect of dispersion on long-range inspection using ultrasonic guided waves, NDT and E Int. 34 (1) (2001) 1–9.
[28] W. Zhu, J. Rose, J. Barshinger, V. Agarwala, Ultrasonic guided wave NDT for hidden corrosion detection, J. Res. Nondestr. Eval. 10 (4) (1998) 205–225.
[29] B. Xu, Z. Shen, X. Ni, J. Lu, Numerical simulation of laser-generated ultrasound by the finite element method, J. Appl. Phys. 95 (4) (2004) 2116–2122.
[30] H. Jeong, M.-C. Park, Finite-element analysis of laser-generated ultrasounds for wave propagation and interaction with surface-breaking cracks, Res. Nondestr. Eval. 16 (1) (2005) 1–14.
[31] P.S. Lowe, R.M. Sanderson, N.V. Boulgouris, A.G. Haig, W. Balachandran, Inspection of cylindrical structures using the first longitudinal guided wave mode in isolation for higher flaw sensitivity, IEEE Sens. J. 16 (3) (2016) 706–714.
[32] A. Cruzado, M. Urchegui, X. Gómez, Finite element modeling of fretting wear scars in the thin steel wires: application in crossed cylinder arrangements, Wear 318 (1) (2014) 98–105.
[33] B. Zhang, C. Ye, B. Liang, Z. Zhang, Y. Zhi, Ductile failure analysis and crack behavior of X65 buried pipes using extended finite element method, Eng. Fail. Anal. 45 (2014) 26–40.
[34] N.K. Mandal, Ratchetting of railhead material of insulated rail joints (IRJs) with reference to endpost thickness, Eng. Fail. Anal. 45 (2014) 347–362.
[35] J.D. Gardner, A. Vijayaraghavan, D.A. Dornfeld, Comparative study of finite element simulation software, 2005.
[36] J. Wang, Z. Shen, B. Xu, X. Ni, J. Guan, J. Lu, Numerical simulation of laser-generated ultrasound in non-metallic material by the finite element method, Opt. Laser Technol. 39 (4) (2007) 806–813.
[37] D. Cerniglia, G. Garcia, S. Kalay, F. Prior, Application of laser induced ultrasound for rail inspection, Proceedings of the World Congress in Railway Research. Montreal, Canada, 2006.
[38] I. Bartoli, F.L. di Scalea, M. Fateh, E. Viola, Modeling guided wave propagation with application to the long-range defect detection in railroad tracks, NDT and E Int. 38 (5) (2005) 325–334.
[39] C. Campos-Castellanos, Y. Gharaibeh, P. Mudge, V. Kappatos, The application of long range ultrasonic testing (LRUT) For examination of hard to access areas on railway tracks, in: Railway Condition Monitoring and Non-Destructive Testing (RCM 2011), 5th IET Conference on, IET, 2011, pp. 1–7.
[40] R.L. Kuhlemeyer, J. Lysmer, Finite element method accuracy for wave propagation problems Tech Rpt J. Soil Mech. Found. Div. 99 (1973).